Publ. Astron. Soc. Aust., 1998, 15, 111–17

Cosmological Applications of Hα Surveys

David Valls–Gabaud[1,2]

[1]UMR CNRS 7550, Observatoire de Strasbourg,
11 Rue de l'Université, 67000 Strasbourg, France
[2]Royal Greenwich Observatory, Madingley Road, Cambridge CB3 0EZ, UK
dvg@astro.u-strasbg.fr

Received 1997 November 15, accepted 1997 December 15

Abstract: We briefly review three main applications of Hα surveys in cosmology, namely: (1) the diffuse Hα emission as a tracer of the free–free foreground that contaminates the fluctuations in the cosmic microwave background radiation; (2) the Hα emission from galaxies as a measure of the formation rate of massive stars, both at low and high redshift; and (3) the diffuse Hα emission from ionised clouds as a constraint on the local ionising background radiation.

Keywords: cosmology: CMBR fluctuations, ionising background radiation — galaxies: star formation rate

1 Diffuse Hα Emission and CMBR Fluctuations

With the advent of dedicated satellites that will make precision measures of the fluctuations of the cosmic microwave background radiation (CMBR) over the whole sky, the next decades will see an attempt to measure the cosmological parameters from these fluctuations with high precision, provided some hypotheses are made (nature of the dark matter, history of the reionisation, etc.). Although the present data are encouraging (see Lineweaver et al. 1997), one of the main limitations will come from our ignorance of the properties of the different contaminating foregrounds. Besides the contamination by galaxies, however, the known Galactic foregrounds (dust, synchrotron and free–free emission) have different spectral properties and spatial morphologies, and hence can be disentangled from the intrinsic, cosmological fluctuations. Figure 1 summarises the expected behaviour of these foregrounds and compares them with the levels of the monopole, dipole and quadrupole moments. Clearly, at the quadrupole level the foregrounds are a major contamination.

Below 10 GHz, the Galactic diffuse emission is dominated by the synchrotron emission from relativistic cosmic rays interacting with Galactic magnetic fields. If the energy distribution of the electron population is a power law, $N(E)dE \propto E^{-\delta}dE$, then the synchrotron spectrum of the ensemble is also a power law. The corresponding brightness temperature scales as $T_b(\nu) \sim \nu^{-(\delta+3)/2}$ so that for a typical energy slope $\delta \sim 2\cdot5$ for electrons between 2 and 15 GeV (corresponding to radiation between 408 MHz and 10 GHz), the spectral slope is approximately $-2\cdot7$. The actual distribution on the sky depends of course on the distribution of the magnetic field, as well as the electron density along the line of sight. For instance, near the Galactic centre, the spectral indices cover the range $-2\cdot2$ to $-1\cdot9$ (Yusef-Zadeh 1989), and so even though steep spectra may be associated with synchrotron emission, flatter energy distributions may be more ambiguous. Currently the only way to quantify the contribution of the synchrotron emission is using the maps at 408 MHz (Haslam et al. 1982) or $1\cdot42$ GHz (Reich & Reich 1988), but their angular resolution is too coarse for the smaller angular scales we are interested in. Extrapolation at both smaller scales and higher frequencies is tricky (e.g. Platania et al. 1997 for a steepening of the spectrum).

At the bottom of the 'valley' of minimum foreground contamination, the free–free emission is the major contribution, and is the least known. Because the Balmer Hα line originates from the same recombinations of ionised gas as the Bremsstrahlung emission, one could use an all-sky Hα survey to trace the free–free contamination. Since there is much confusion in the present literature concerning the precise relation between the Hα and the Bremsstrahlung emissions (mainly due to different underlying approximations), we derive here accurate expressions. These are important because we are looking for fluctuations in the residuals, rather than simple proportions.

The absorption cross section for a free–free transition from E_i to E_j for an ion of charge Z by an electron with initial velocity v is given by the classical (Kramers) cross section times a Gaunt cofactor (e.g. Oster 1961)

$$d\sigma_{ff} = \frac{4\pi^6}{3\sqrt{3}hcm_e^2}\left(\frac{Z^2}{\nu^3}\right)\left(\frac{g_{ff}(n_i,n_f)}{v}\right)dv\,, \quad (1)$$

1323-3580/98/010111$05.00

https://doi.org/10.1071/AS98111 Published online by Cambridge University Press

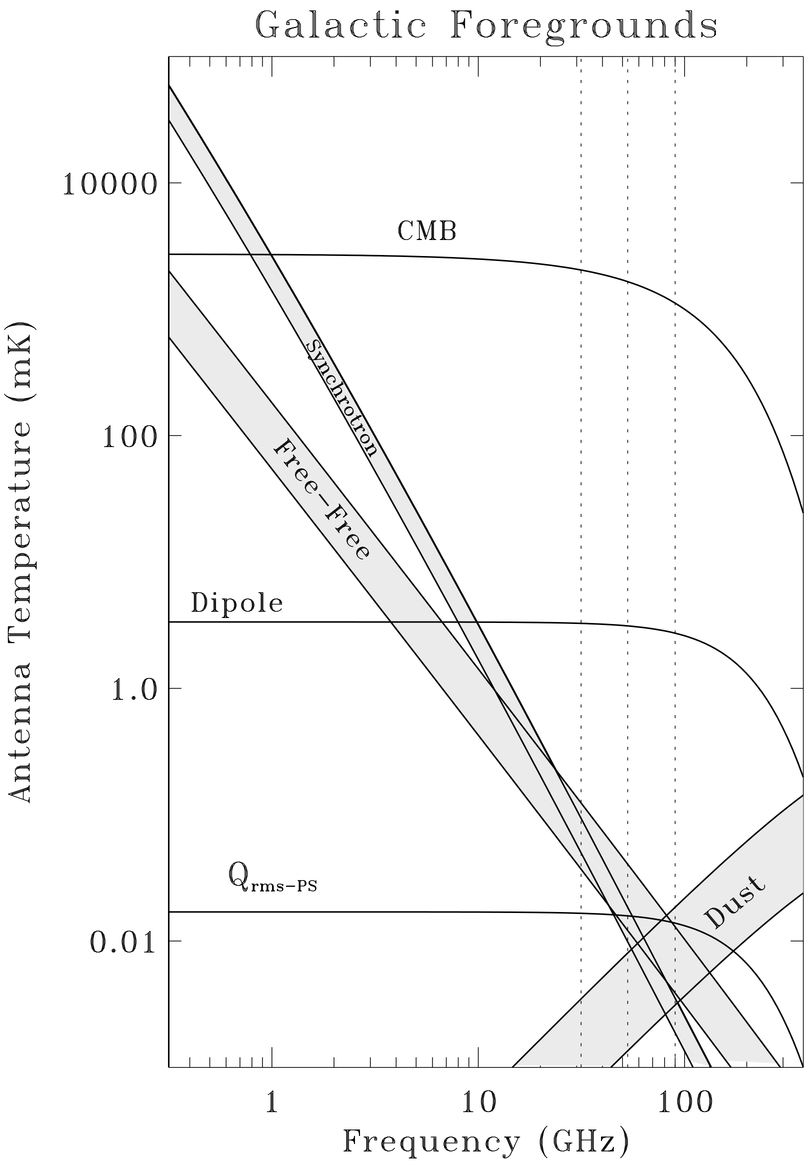

Figure 1—Comparison of the expected frequency dependence of foregrounds with the monopole, dipole, and quadrupole levels of the CMBR. The diffuse emission from dust dominates above 80 GHz, while synchrotron emission dominates below 20 GHz. The Bremsstrahlung is likely to contaminate the fluctuations observed between 20 and 80 GHz. The dashed vertical lines indicate the channels used in the DMR experiment on COBE (31·5, 53 and 90 GHz).

where $n_{i,f} = Z^2\mathrm{Ry}/E_{i,f}$ and $h\nu/Z^2\mathrm{Ry} = n_f^{-2} - n_i^{-2}$. The total absorption cross section per ion and per electron is obtained by summing over all incident electron velocities, assuming a Maxwell–Boltzmann distribution,

$$N_e(v)dv = 4\pi N_e \left(\frac{m_e}{2\pi kT}\right)^{\frac{3}{2}} \times v^2 \exp\left(\frac{-m_e v^2}{2kT}\right) dv\,, \qquad (2)$$

so that

$$\sigma_{ff} = \left(\frac{4e^6}{3ch}\right)\left(\frac{2\pi}{3km_e^3}\right)^{\frac{1}{2}} \times T^{-1/2}\,\frac{Z^2 \bar{g}_{ff}(\gamma^2, u)}{\nu^3}\,. \qquad (3)$$

The thermal average is

$$\bar{g}_{ff}(\gamma^2, u) = \int_0^\infty g_{ff}(n_i(t), n_f(t))\, e^{-t}\, dt\,, \qquad (4)$$

where $t = m_e v^2/2kT$, $n_i(t) = \gamma/\sqrt{t}$, $n_f(t) = \gamma/(u+t)^{\frac{1}{2}}$, $\gamma^2 = Z^2\mathrm{Ry}/kT$ and $u = h\nu/kT$.

The crux of the problem is the evaluation of the Gaunt factor, for which several approximations exist, depending upon the regime where the electron–ion collisions take place. For temperatures below $2{\times}10^4$ K, and a frequency range between 1 and 1000 GHz, that is $\gamma^2 \sim 10$ and $u \leq 0{\cdot}01$, the classical, small-angle, long-wavelength approximation is appropriate (see e.g. Novikov & Thorne 1973):

https://doi.org/10.1071/AS98111 Published online by Cambridge University Press

$$\bar{g}_{ff}(\gamma^2, u) = -\frac{\sqrt{3}}{\pi}\ln\left[4\zeta^{\frac{5}{2}}u\gamma\right]$$
$$= 0\cdot5513\ln\left(T^{1\cdot5}/Z\nu\right) + 9\cdot75\,, \quad (5)$$

where $\zeta = 1\cdot781072...$ is Euler's constant. One can write this approximately as $\bar{g}_{ff} \approx g_0 T^a \nu^b$, and by noting that $d\bar{g}_{ff}/d\nu = b\bar{g}_{ff}/\nu \approx -0\cdot5513/\nu$, $d\bar{g}_{ff}/dT = a\bar{g}_{ff}/T = 0\cdot82695/T$, for $Z = 1$,

$$\bar{g}_{ff} \approx 4\cdot4\left(\frac{T}{10^4\,\mathrm{K}}\right)^{0\cdot21}\left(\frac{\nu}{40\,\mathrm{GHz}}\right)^{-0\cdot14}. \quad (6)$$

But in fact the 'effective' spectral slope changes from about $-0\cdot08$ at 1 GHz to $-0\cdot18$ at 1000 GHz, and in any case these expressions give errors up to 20% at the high-frequency range. A more convenient approximation, based on a bi-dimensional Chebyshev fit, was given by Hummer (1988) with a maximum relative error of $0\cdot7$%. Again, this new approximation is only valid above 10–40 GHz, given the likely temperature range.

Since Bremsstrahlung emission is a purely collisional process, and hence in LTE, $S_\nu = B_\nu$, but stimulated emission must be taken into account for the final, thermally averaged absorption coefficient,

$$\kappa_\nu = \left(\sum_{\mathrm{ion}}\sigma_{ff}N_{\mathrm{ion}}N_e\right)\left[1 - e^{-h\nu/kT}\right]. \quad (7)$$

The final intensity is then

$$I_\nu = \frac{8e^6}{3c^3}\left(\frac{2\pi}{3km_e^3}\right)^{\frac{1}{2}}\frac{1}{T^{\frac{1}{2}}}\,e^{-h\nu/kT}$$
$$\times\sum_{\mathrm{ion}} Z^2\,\bar{g}_{ff}(Z,\nu,T)\,N_e N_{\mathrm{ion}}\,. \quad (8)$$

At long wavelengths, the stimulated emission correction dominates, $1 - e^{-h\nu/kT} \approx h\nu/kT$, and the exponential in the previous equation becomes unity (as would be obtained by substituting the Rayleigh–Jeans approximation for the source function). Since under normal photoionisation conditions the dominant ions will be HII and HeII, sharing the same $Z = 1$, the Gaunt factor comes out of the sum. The emission measure contributed by helium is most uncertain. The upper limits on the emission of the HeI λ5876 recombination line (Reynolds & Tufte 1995) indicates that most of the He has to be neutral. However, new observations detect the line (Rand 1997; Greenawalt, Walterbos & Braun 1997; Martin & Kennicutt 1997 Reynolds et al. 1998, present issue p. 14) indicating not only that HeII is clearly present, but also that He could perhaps be fully ionised, although further measures are required. What is really needed to quantify the Bremsstrahlung emission is the measure of ionisation degree in the diffuse ISM along the different lines of sight, via the detection of several metal lines sensitive to temperature and density.

The Balmer α emission is also proportional to the emission measure, since it is a fraction of the total number of recombinations. It also depends on whether the Lyman continuum is optically thin (case A) or not (case B). Fitting the emission coefficients for Hβ given by Brocklehurst (1972) and Martin (1988), and the Balmer decrement Hα/Hβ for the temperature range from 5000 to 20,000 K, we get

$$I(H\alpha) \overset{\mathrm{CaseB}}{=} 9\cdot41\times10^{-8}\,T_4^{-1\cdot017}\,10^{-0\cdot029/T_4}$$
$$\times\left(\frac{EM}{\mathrm{cm}^{-6}\,\mathrm{pc}}\right)\mathrm{erg\,cm^{-2}\,s^{-1}\,sr^{-1}} \quad (9)$$

and

$$I(H\alpha) \overset{\mathrm{CaseA}}{=} 6\cdot36\times10^{-8}\,T_4^{-1\cdot134}\,10^{-0\cdot038/T_4}$$
$$\times\left(\frac{EM}{\mathrm{cm}^{-6}\,\mathrm{pc}}\right)\mathrm{erg\,cm^{-2}\,s^{-1}\,sr^{-1}}\,. \quad (10)$$

A useful expression is then the brightness temperature of the free–free emission associated with the emission of one Rayleigh in Hα, assuming the same emission measure. Since $T_b = 2\nu^2 I_\nu/c^2$, we have for Case B recombination

$$\frac{T_b(\mu\mathrm{K})}{I_{H\alpha}(\mathrm{R})} \approx 14\cdot0\,T_4^{0\cdot317}\,10^{+0\cdot029/T_4}$$
$$\times\left(1 + 0\cdot08\frac{\chi_{\mathrm{HeII}}}{\chi_{\mathrm{He}}}\frac{n_{\mathrm{He}}}{0\cdot08}\right)\frac{Z^2\,\bar{g}_{ff}(\nu,T)}{\nu_{10}^2}\,, \quad (11)$$

where ν_{10} is the frequency in units of 10 GHz, and n_{He} is the abundance of helium by number (see Figure 2). The usefulness of this technique is limited by at least two factors. First, the dust present along the line of sight will decrease the Hα surface brightness. Correlations between the IRAS 100 μm and DIRBE 240 μm maps could help to explain possible partial correlations between these maps and the diffuse Hα emission. Second, the temperature could be much higher, and so decrease the number of optical recombinations to undetectable levels, and at the same time increase the contribution from helium to the Bremsstrahlung emission. Despite these caveats, there have been a few attempts to measure the fluctuations in the Hα brightness in the North Celestial Pole (Simonetti, Dennison & Topasna 1996; Gaustad, McCullough

https://doi.org/10.1071/AS98111 Published online by Cambridge University Press

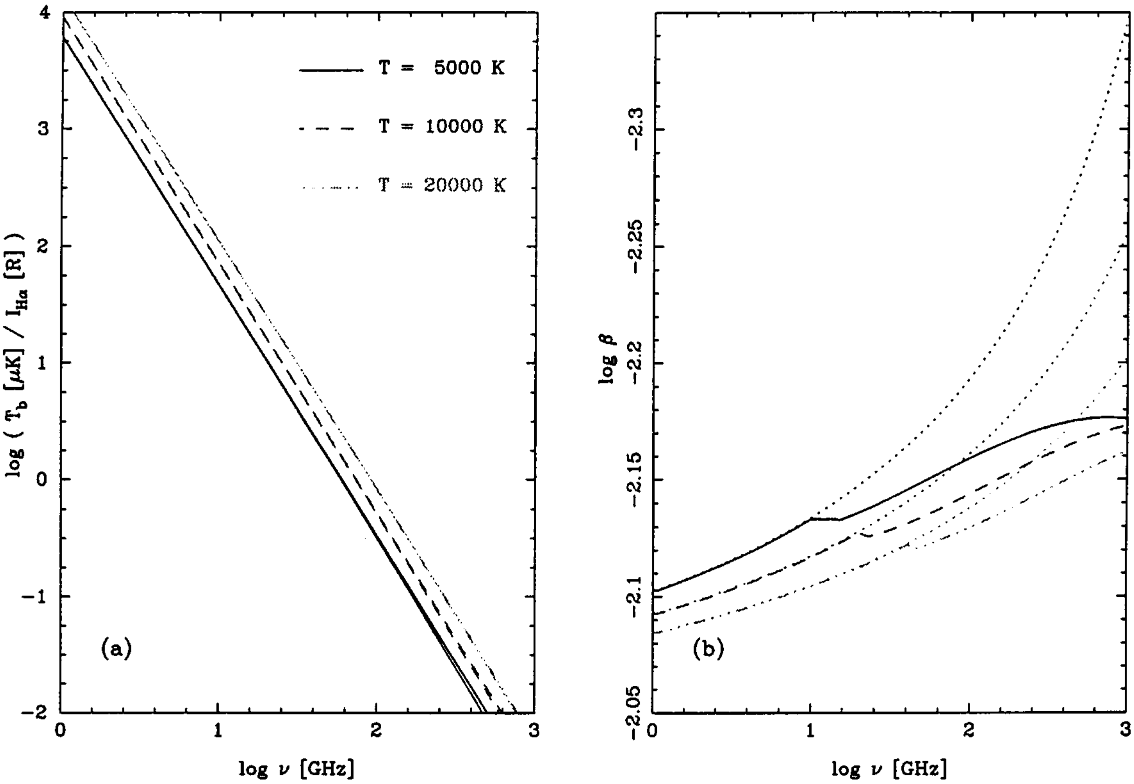

Figure 2—Predicted brightness temperature of the free–free emission associated with the emission of 1 Rayleigh in Balmer α, assuming a common emission measure. (a) Brightness temperature for several gas temperatures; (b) spectral slope of the Bremsstrahlung emission with two different approximations for the thermal average of the Gaunt factor: long-wavelength (dotted lines), Hummer (1988) bi-dimensional Chebyshev fit [same lines as panel (a)]. The small discontinuities are due to the transition between the two approximations.

& Van Buren 1996). The limitation of these narrow-bandpass filter observations is that most of the signal comes in fact from the geocoronal emission, which needs to be subtracted with high accuracy. Alternatively, one could use Fabry–Perot observations to separate this line from the diffuse Hα emission. A collaboration between the Strasbourg and Marseilles observatories, using the CIGALE interferometer at La Silla, observed some of the fields measured by the CMBR South Pole experiment (Schuster et al. 1991; Gundersen et al. 1994) where an excess temperature was reported. Figure 3 presents some of the scans, and shows that very little diffuse emission (less than 0·2 Rayleigh) is present between the geocoronal Hα line and the night-sky OH line. These small residuals cannot explain the anomalous component seen in several experiments, provided the assumptions made above in relating Hα and Bremsstrahlung apply.

Above 100 GHz, the emission is dominated by cold dust, and the IRAS 100 μm and DIRBE 240 μm maps are useful indicators of the expected contamination level. Recent analysis of the COBE/DMR data shows a significant correlation between the CMBR fluctuations and the DIRBE maps in the North Polar spur area (Kogut et al. 1996a,b), and the comparison of the Saskatoon maps with IRAS also presents some correlation (De Oliveira-Costa et al. 1997; Leitch et al. 1997). This is all the more surprising because the frequencies selected, around 40 GHz, should be more sensitive to the Bremsstrahlung emission than to the dust foreground (see Figure 1). A recent alternative has been suggested by Draine & Lazarian (1997), where spinning dust grains would produce a significant emission up to 10 GHz, but given the patchy nature of the WIM, it is unlikely that the correlation extends on all scales (see also Gutierrez de la Cruz et al. 1995; McCullough 1997; Kogut 1997; Kowitt et al. 1997).

2 Star Formation Rate of Massive Stars

The proportionality between the emission measure and the intensity of the Balmer Hα emission provides an estimate of the total number of ionising photons emitted, and hence on the number of massive, hot stars that produced them. This has become the standard technique to infer not only the star formation rate but also the initial mass function (IMF) of massive stars. The total number of ionising photons in a stellar population of age t, with an IMF $\phi(m)$, and with a history of SFR given by $\Psi(t)$, can be expressed as

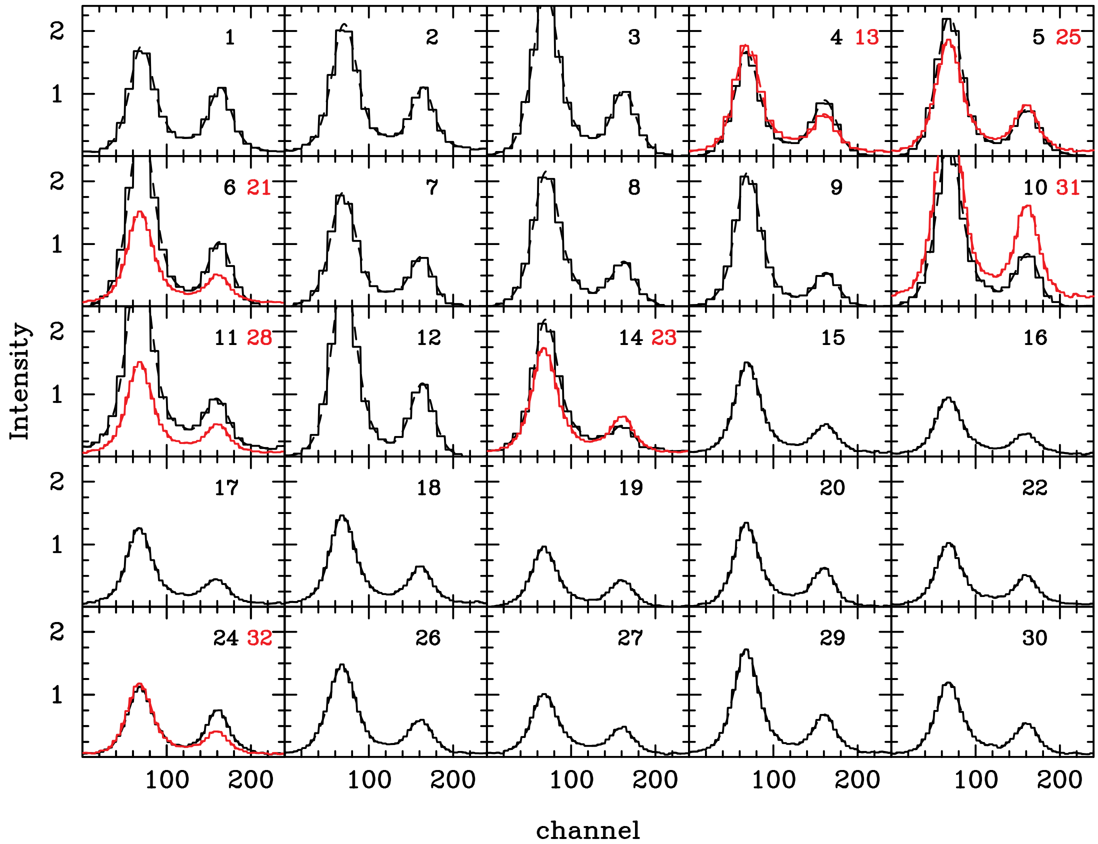

Figure 3—Sample Fabry–Perot scans for 25 South Pole fields observed by the Strasbourg–Marseille collaboration. Note the very small residual levels between the geocoronal Hα and sky OH λλ6568·77, 6568·78 Å lines.

$$N_{\mathrm{Ly-c}}(t) = \int_{m_{\mathrm{eff}}}^{m_{\mathrm{up}}} dm \int_0^{\tau(\mathrm{TAMS})} \Psi(t-\tau)\,\phi(m) \times N_{\mathrm{Ly-c}}(m,\tau)d\tau\,, \tag{12}$$

where $N_{\mathrm{Ly-c}}(m,\tau)$ is the number of ionising photons emitted by stars of mass m at time τ, and the effective lifetime extends from the ZAMS to the terminal age main sequence (TAMS). Note that the effective cutoff mass m_{eff} is given by the IMF-weighted Ly–c production rate, and is about 10 $\mathrm{M}_\odot$. The reason for this is that the dependence of the number of emitted ionising photons with temperature (mass) is extremely steep: going from 20,000 K to 35,000 K increases the Ly–c flux density by 4 orders of magnitude. This sharp cutoff, weighted by the IMF, makes sure that no stars below about 10 $\mathrm{M}_\odot$ contribute to the final ionising flux. This implies that estimates of the ionising flux give a *direct* constraint on the IMF of stars above 10 $\mathrm{M}_\odot$, but says nothing on the IMF below that mass. Using the recent models from Schaerer & De Koter (1997), which incorporate for the first time stellar interiors with realistic stellar atmospheres, we obtain for a Salpeter IMF

$$\left(\frac{N_{\mathrm{Ly-c}}}{10^{56}\,\mathrm{s}^{-1}}\right) = 3\cdot 1\left(\frac{\Psi}{M_\odot\,\mathrm{yr}^{-1}}\right) \times \left(\frac{0\cdot 1 - 1\cdot 5 m_{\mathrm{up}}^{-0\cdot 66} + 8\cdot 6 m_{\mathrm{up}}^{1\cdot 66}}{m_{\mathrm{low}}^{-0\cdot 35} - m_{\mathrm{up}}^{-0\cdot 35}}\right). \tag{13}$$

The existence of m_{low} in the equation above is only the consequence of the assumption of continuity (à la Salpeter) of the IMF below 10 solar masses. Under standard (case B) recombination conditions, the ratio $\Psi/L(H\alpha)$ is approximately $2\cdot 2^{+2\cdot 5}_{-1\cdot 5} \times 10^{-8}\,\mathrm{M}_\odot\mathrm{yr}^{-1}\mathrm{L}_\odot^{-1}$, for a wide range of IMF slopes.

However, estimating the flux of ionising photons from the Hα emission has several problems: (1) the ionisation conditions for the opacity in the Lyman continuum (clumpy ISM, escape fraction, diffuse emission); (2) dust corrections (at wavelengths below 912 Å dust tends to absorb rather than to scatter); (3) contamination by the [NII] λ6583 line (variable, and usually not resolved from Hα); (4) evolution of the stellar populations (which may produce an underlying absorption Hα line); and (5) contamination of the Hα line by nonthermal processes (presence of AGN-like activity).

https://doi.org/10.1071/AS98111 Published online by Cambridge University Press

Each of these caveats would deserve a section by itself, but we will comment here only on the first one, which has implications for the next section. Oey & Kennicutt (1997) compared Hα fluxes with predicted Ly–c fluxes and found that a significant fraction (up to 51%) could leak from HII regions, providing a bath of ionising photons in the WIM. The origin of these Ly–c photons could either be from the leakage in HII regions or from field massive stars. The first interpretation is favoured by Ferguson et al. (1996a, b), although Patel & Wilson (1995a, b) argue that the number of OB stars detected in the field is more than enough to ionise the WIM. In any case, the failure to take into account the diffuse Hα emission underestimates the true SFR by factors between about 3 and an order of magnitude.

In the case of an ensemble of galaxies, there is, in addition, the problem of the completeness of the sample, and of the temporal evolution of the emission line due to the evolving stellar populations on cosmological timescales. Despite these caveats, useful constraints can be obtained on the luminosity density at Hα (assuming that the observations are sensitive enough to low fluxes that the luminosity density converges). For instance, Tresse & Maddox (1997) obtained a luminosity density of $3{\cdot}16{\times}10^{39}$ erg s^{-1} Mpc^{-3} at $\langle z\rangle \sim 0{\cdot}2$ using the CFRS sample, which is substantially larger than the local value. For higher redshifts the sensitivity in the near IR is much lower, and the current limits (van der Werf, in preparation) are about $1{\cdot}56{\times}10^{39}$ erg s^{-1} Mpc^{-3} at $\langle z\rangle \sim 2{\cdot}25$, much lower than the (lower) limits obtained from the HDF survey.

3 Local Ionising Background Radiation

From the studies of the WIM in our Galaxy and in nearby galaxies, it appears likely that a substantial fraction of ionising photons could escape from galaxies. Although at first surprising, the high escape fraction may be due to the patchy, clumpy nature nature of the ISM, fractal (Elmegreen 1997) or otherwise. Disk photons reach the Reynolds layer. Within the inner 60 kpc or so, the detection of diffuse Hα in the Magellanic Stream (Weiner & Williams 1996) implies that a large fraction of galactic ionising photons reach that distance (Bland-Hawthorn & Maloney 1998), while in nearby dwarf galaxies the large number of expanding cavities which may be fully ionised certainly allows a large fraction of ionising photons to escape from these low-opacity regions (e.g. Puche et al. 1992; Puche & Westpfahl 1994). An obvious test is to take integrated spectra of these galaxies at wavelengths around 912 Å. This has been attempted with HUT on a few nearby starburst galaxies, with apparently negative results (Leitherer et al. 1995). However, the inclusion of the Galactic absorption, important for the low-redshift galaxies studied, increased the escaping fraction, and *lower* limits ranging from 3% to 57% are allowed (Hurwitz, Jelinsky & van Dyke Dixon 1997).

If many ionising photons escape from galaxies, they will contribute significantly to the ionising background radiation, which is usually thought to be dominated by quasars. Yet locally quasars contribute much less than 10% to the luminosity density in the B and U bands. Could galaxies dominate the background, at least locally? Again the proportionality between the emission measure, the number of recombinations and the Hα emission give a useful constraint on the local ionising background, as first pointed out by Sunyaev (1969). Assuming that the Hα is optically thin, the ionising photon flux is

$$\Phi_{\rm ion} = \pi \int_{\nu_L}^{\infty} \frac{J_\nu}{h\,\nu} d\nu = \frac{4\pi\alpha_{\rm tot}}{\epsilon(H\alpha)} \frac{I(H\alpha)}{h\,\nu} \frac{A_\perp}{A_{\rm tot}}\,, \tag{14}$$

where $\alpha_{\rm tot}$ and $\epsilon(H\alpha)$ are the total recombination coefficient and the Hα emission rate respectively, and the aspect ratio of projected to total area, $A_\perp/A_{\rm tot}$, goes from 1/2 for a two-sided slab to 1/4 for a sphere. This expression actually assumes that the ionisation comes only from one side, the general expression for the ionisation from both sides not having been solved yet. The observations of isolated extragalactic clouds (e.g. Stocke et al. 1991; Vogel et al. 1995) provide limits of about $3{\times}10^4$ ionising photons s^{-1} cm^{-2}, which becomes a limit on the ionising background at the Lyman limit of $J_{\nu_L} < 8 \times 10^{-23}$ erg s^{-1} cm^{-2} Hz^{-1} sr^{-1}, assuming a slope of $1{\cdot}4$ for the background, typical for quasars. These values also assume case B recombination. However, as shown elsewhere (Valls–Gabaud & Vernet 1998), galaxies are the main component of the ionising background, and their soft spectra are consistent with the pattern of ionisation traced by Si IV, Si III, C IV, C III observed at $z > 3$. The consequence of this model is that at low redshift the background is also very soft, with an effective slope of the order of 3 or more. This relaxes the constraint on the amplitude of the background, since

$$J_\nu = J_{\nu_L} \left(\frac{\nu}{\nu_L}\right)^{-\alpha} \Longrightarrow J_{\nu_L} = \frac{\alpha h}{\pi}\, \Phi_{\rm ion}\,. \tag{15}$$

Then the limit becomes $J_{\nu_L} < 5{\cdot}6 \times 10^{-22}$ erg s^{-1} cm^{-2} Hz^{-1} sr^{-1} for case A recombination, which is more appropriate. Deharveng et al. (1997) obtained strong upper limits on the escape fraction using the Hα luminosity density at $z = 0$, but assuming a background dominated by quasars. With a galaxy-dominated background, the present limits are consistent with an average escaping fraction larger

https://doi.org/10.1071/AS98111 Published online by Cambridge University Press

than 30%. The model predicts that the local background must be very soft, and hence can be falsified because low ionisation stages must prevail over high ionisation species in isolated extragalactic clouds.

Acknowledgments

It is a pleasure to thank my collaborators on these topics, and particularly J. Bartlett, P. Amram, M. Marcelin and J. Vernet for letting me mention some of our recent results here. I thank R. Reynolds, S. Nossal and D. Schaerer for interesting discussions. I am grateful to the organisers for financial support and to Prof. B. McAdam and his family for their friendly hospitality.

Bland-Hawthorn, J., & Maloney, P. 1998, ApJ, in press
Brocklehurst, M. 1972, MNRAS, 157, 211
De Oliveira-Costa, A., et al. 1997, ApJ, 482, L17
Deharveng, J. M., Faïsse, S., Milliard, B., & LeBrun, V. 1997, A&A, 325, 1259
Draine, B. T., & Lazarian, A. 1997, ApJ, submitted
Elmegreen, B. G. 1997, ApJ, 477, 196
Ferguson, A. M. N, Wyse, R. F. G., Gallagher, J. S., & Hunter, D. A. 1996a, AJ, 111, 2265
Ferguson, A. M. N, Wyse, R. F. G., & Gallagher, J. S. 1996b, AJ, 112, 2567
Gaustad, J. E., McCullough, P. R., & Van Buren, D. 1996, PASP, 108, 351
Greenawalt, B., Walterbos, R. A. M., & Braun, R. 1997, ApJ, 483, 666
Gundersen, J. O., et al. 1995, ApJ, 443, L57
Gutierrez de la Cruz, C. M., et al. 1995, ApJ, 442, 10
Haslam, C. G. T., Salter, C. J., Stoffel, H., & Wilson, W. E. 1982, A&AS, 47, 1
Hummer, D. G. 1988, ApJ, 327, 477
Hurwitz, M., Jelinsky, P., & van Dyke Dixon, W. 1997, ApJ, 481, L31
Kogut, A. 1997, AJ, 114, 1127
Kogut, A., et al. 1996a, ApJ, 460, 1
Kogut, A., et al. 1996b, ApJ, 464, L5
Kowitt, M. S., et al. 1996, ApJ, 482, 17
Leitch, E. M., Readhead, A. C. S., Pearson, T. J., & Myers, S. T. 1997, ApJ, 486, L23
Leitherer, C., et al. 1995, ApJ, 454, L19
Lineweaver, C. H., Barbosa, D., Blanchard, A., & Bartlett, J. G. 1997, A&A, 322, 365
Martin, C. L., & Kennicutt, R. C. 1997, ApJ, 483, 698
Martin, P. G. 1988, ApJS, 66, 125
McCullough, P. R. 1997, AJ, 113, 2186
Novikov, I. D., & Thorne, K. S. 1973, in Black Holes, ed. C. DeWitt & B. S. DeWitt (New York: Gordon & Breach), p. 343
Oey, M. S., & Kennicutt, R. C. 1997, MNRAS, 291, 827
Oster, L. 1961, Rev. Mod. Phys., 33, 525
Patel, K., & Wilson, C. D. 1995a, ApJ, 451, 607
Patel, K., & Wilson, C. D. 1995b, ApJ, 453, 162
Platania, P., et al. 1997, ApJ, submitted (astro-ph 9707252)
Puche, D., et al. 1992, AJ, 103, 1841
Puche, D., & Westpfahl, D. 1994, in ESO/OHP Workshop on Dwarf Galaxies, ed. G. Meylan & P. Prugniel (Garching: ESO), p. 273
Rand, R. J. 1997, ApJ, 474, 129
Reich, P., & Reich, W. 1988, A&AS, 74, 7
Reynolds, R. J., & Tufte, S. L. 1993, ApJ, 439, L17
Reynolds, R. J., Tufte, S. L., Haffner, L. M., Jaehnig, K., & Percival, J. W. 1998, PASA, 15, 14
Schaerer, D., & De Koter, A. 1997, A&A, 322, 598
Schuster, J., et al. 1993, ApJ, 412, L47
Simonetti, J. H., Dennison, B., & Topasna, G. A. 1996, ApJ, 458, L1
Stocke, J. T., et al. 1991, ApJ, 374, 72
Sunyaev, R. 1969, ApJ Lett., 3, 33
Tresse, L., & Maddox, S. J. 1997, ApJ, in press
Vogel, S. N., et al. 1995, ApJ, 441, 162
Valls-Gabaud, D., & Vernet, J. 1998, MNRAS, submitted
Weiner, B. J., & Williams, T. B. 1996, AJ, 111, 1156
Yusef-Zadeh, F. 1989, in The Center of the Galaxy, ed. M. Morris (Dordrecht: Kluwer), p. 243

https://doi.org/10.1071/AS98111 Published online by Cambridge University Press